Reciprocal space maps of PbTe/SnTe superlattices

S. O. Ferreira,[a] E. Abramof, P. H. O. Rappl, A. Y. Ueta, H. Closs, C. Boschetti, P. Motisuke, and I. N. Bandeira
Instituto Nacional de Pesquisas Espaciais-INPE. Laboratório Associado de Sensores e Materiais-LAS – CEP, 12201-970 – São José dos Campos, Brazil

(Received 24 March 1998; accepted for publication 1 July 1998)

PbTe/SnTe superlattices were grown on (111) BaF_2 substrates by molecular beam epitaxy using PbTe as buffer layers. The individual layer thickness and number of repetitions were chosen in order to change the strain profile in the superlattices from completely pseudomorphic to partially relaxed. The superlattices structural properties were investigated by making reciprocal space maps around the asymmetric (224) Bragg diffraction points and $\omega/2\Theta$ scans for the (222) diffraction with a high resolution diffractometer in the triple axis configuration. With the strain information obtained from the maps, the (222) $\omega/2\Theta$ scan was simulated by dynamical diffraction theory. The simulated spectra of the pseudomorphic superlattices, in which the in-plane lattice constant is assumed to be the same as the PbTe buffer throughout the superlattice, fitted in a remarkably good agreement with the measured data, indicating that almost structurally perfect samples were obtained. For the thicker superlattices, the (224) reciprocal space maps revealed a complex strain profile. Our results show the importance of detailed structural characterization on the interpretation of the electrical properties. [S0021-8979(98)03219-8]

I. INTRODUCTION

The study of the PbTe–SnTe alloy system has attracted much interest due to their application for infrared detectors moreover due to many interesting features as compared to III–V or II–VI semiconductors. The main properties are: (i) the inversion of valence and conduction band symmetry between PbTe and SnTe, which, in principle, produces a zero gap compound for Sn composition around 35% at $T=0$ K; (ii) very large dielectric constant and therefore high carrier mobility due to screening; (iii) direct energy gap at the L points of the Brillouin zone with many valleys; (iv) a type II alignment of the band edges, with the valence band maximum of SnTe higher than the conduction band minimum of PbTe. Many authors have studied the electrical properties of PbTe/SnTe superlattices (SLs) grown on BaF_2 (111) and KCl (001) substrates in the last ten years.[1–3] Murase *et al.*[1] have observed a superconducting transition at temperatures varying from 1.5 to 7 K, depending on PbTe layer thickness and sample substrate, and suggested that the phenomena are related with the presence of metal microprecipitates in the samples. Mironov *et al.*[3] have explained the anomalous behavior of the conductivity in their samples by a structural phase transition undergone by the SnTe layer. Litvinov *et al.*[4] have used the presence of two-dimensional interface states to explain the magnetic field dependence of Hall coefficient of short-period SLs. Unfortunately, structural characterization of these samples has been almost forgotten, although many of the observed electrical properties and most of the open questions are probably related to structural details of the samples. The main problem in these structures is related with the high lattice parameter mismatch between PbTe, SnTe, and the substrate. The strain produced by this mismatch will change the band alignment of the layers and influence all electrical properties of the SL.

In this paper we focus our attention on the structural properties of PbTe/SnTe superlattices. The samples have been grown using solid source molecular beam epitaxy (MBE). Detailed structural characterization has been made by high-resolution x-ray diffraction. Reciprocal space maps of asymmetric diffraction peaks, measured using a triple axis configuration offer information about the sample strain state, which can be used as input parameters for the dynamical simulation of the experimental x-ray spectra.

II. SAMPLE GROWTH

The superlattices were grown in a RIBER 32P MBE system equipped with PbTe, SnTe, and Te effusion cells. As substrates, we have used freshly cleaved BaF_2 (111) crystals, which were preheated at 500 °C for 15 min before growth. The growth temperature was 250 °C and the growth rate about 4 Å/s. Before growing the superlattices, PbTe and SnTe single layers were grown using stoichiometric sources. These samples have shown very good crystalline quality, with the rocking curve of the (222) diffraction line showing a full width at half maximum (FWHM) of about 100 arcsec, for 4 μm thick layers. The PbTe layers were *p* type with hole concentration of 3×10^{17} cm^{-3} and the SnTe samples were also *p* type with carrier concentration of 2×10^{19} cm^{-3}. Details about growth and characterization of these layers have been published elsewhere.[5,6]

The SLs were grown on the top of 4 μm thick PbTe buffer layers. The growth rates of PbTe and SnTe were checked by measuring the thickness of calibration samples and also by measuring reflection high-energy electron diffraction (RHEED) intensity oscillations. Substrate rotation

[a]On leave to Universidade Federal de Viçosa; electronic mail: sukarno@mail.ufv.br

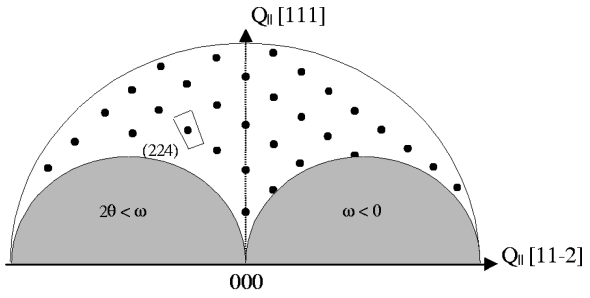

FIG. 1. Schematic representation of the reciprocal lattice points of a (111) oriented PbTe sample, showing a map around the (224) reciprocal lattice point. The shaded areas are not accessible for samples which are not transparent to the x ray.

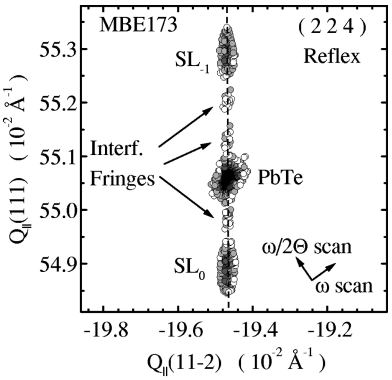

FIG. 2. Reciprocal space map around the (224) asymmetric Bragg diffraction point for a pseudomorphic PbTe/SnTe SL. The nominal PbTe and SnTe thickness are 175 and 17 Å, respectively. The total number of repetitions is seven.

during the growth guarantees the thickness uniformity. The relatively low substrate temperature used (250 °C) was chosen to minimize interdiffusion and ensure abrupt interfaces.

For the analysis of the structural properties, we have grown two types of PbTe/SnTe superlattices. The first one is intended to be completely pseudomorphic to the PbTe buffer layer with the in-plane lattice parameter equal to the lattice parameter of the PbTe throughout the whole SL structure. For this purpose, the thickness of PbTe and SnTe layers are chosen in such a way that the average Sn content in the SL is under 10% and the number of repetitions (less than eight) is calculated in order to maintain the whole SL thickness smaller than the critical thickness of the corresponding PbSnTe layer in relation to the PbTe buffer. In the second type of SLs, the SnTe layer thickness is still below the critical thickness, but the number of repetitions is large so that the superlattice, as a whole, is expected to relax in relation to the buffer. These SLs are called free-standing, having an in-plane lattice constant smaller than the lattice constant of the buffer layer. This second series of SLs consisted of 50 repetitions of PbTe and SnTe layers, with individual thickness ranging from 150 to 300 Å for PbTe and from 20 to 140 Å for SnTe. For SnTe layers thicker than 140 Å, we have observed a rapid decrease in sample quality, as indicated by rocking curve FWHM. This fact agrees with observations of Fedorenko *et al.*,[7] who have measured a critical thickness around 100 Å for SnTe on PbTe. Above this thickness, the strain is relieved by the introduction of misfit dislocations, which cause degradation in crystalline quality.

III. HIGH RESOLUTION X-RAY CHARACTERIZATION

The system used for structural analysis was a Philips X'Pert diffractometer in the triple axis configuration. It employs a four-crystal Ge(220) monochromator in the primary optics, which gives an axial divergence ($\Delta\omega$) of 12 arcsec and a wavelength dispersion of less than 3×10^{-5}. A channel-cut Ge(220) analyzer crystal in the secondary optics gives also a 12 arcsec resolution in the 2Θ direction ($\Delta\Theta$). Recently, a number of authors have described in detail the power of this technique for characterization of heterostructures.[8,9] Figure 1 shows a schematic representation of the reciprocal lattice points of a (111) oriented PbTe layer with x-ray incidence in the [11-2] azimuth. The shaded areas are not accessible, since $\omega<0$ or $2\Theta<\omega$, where ω is the angle between the incident beam and sample surface and 2Θ the angle between the incident and diffracted beam. The horizontal and vertical coordinates, $Q_x=Q_\parallel$ [11-2] and $Q_y=Q_\parallel$ [111], give a measurement of the reciprocal lattice constant parallel (in-plane) and perpendicular (growth direction) to the sample surface, respectively. The area marked in the figure illustrates a map around the asymmetrical (224) diffraction peak. The map is obtained making a series of $\omega/2\Theta$ scans (radial direction) at different ω settings or a series of ω scans (rocking curves, axial direction) at different 2Θ settings. The directions of these scans are also indicated in the figure.

In all maps shown in this paper the x-ray intensity information has been given using a linear grey scale, where the black symbols correspond to intensities above 80% of the maximum intensity and the white symbols to intensities lower than 5%. Although this procedure gives only qualitative information about the intensity distribution, it makes it easier to interpret the maps, since the strain analysis is based only on the position and shape of the reciprocal lattice peaks. Detailed, quantitative information about the intensity variations of each peak is given by the $\omega/2\Theta$ scans.

IV. RESULTS AND DISCUSSION

Figure 2 shows the reciprocal space map around the asymmetrical (224) point for a sample representative of the first series. The sample nominally consists of a 4 μm PbTe buffer and seven repetitions of PbTe and SnTe layers with nominal thickness of 175 and 17 Å, respectively. The map shows the PbTe buffer peak and two superlattice satellite peaks. The three peaks, which appear in between, are interference fringes related to the total superlattice thickness. As can be seen, all peaks in the map (224) have the same horizontal coordinate, indicating that all layers have the same in-plane lattice constant, confirming that this PbTe/SnTe SL is completely pseudomorphic to the PbTe buffer layer. Another important information given from the map is that only the buffer peak has some deformation in the ω direction, what means that all defects are restricted to this layer.

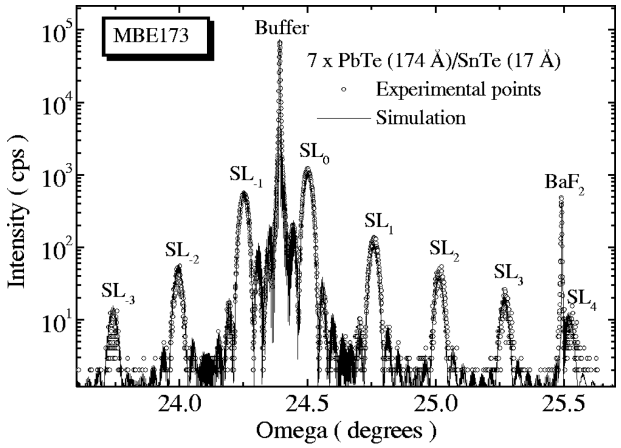

FIG. 3. $\omega/2\Theta$ scan of the (222) diffraction peak for the same sample analyzed in Fig. 2. The solid curve is a dynamical simulation with PbTe and SnTe layer thickness of 174 and 17 Å, respectively. The elastic constants used are the ones published in the literature (see Ref. 10).

In Fig. 3, we see a $\omega/2\Theta$ scan for the (222) diffraction of the same sample. This curve can be seen as a cut through the center of the map in Fig. 2, except for the fact that now we are looking to a symmetric (222) diffraction. As was mentioned previously, with this scan we get all intensity information which is not shown in the map. This spectrum shows the peaks of the BaF_2 substrate and PbTe buffer and 8 SL satellites, besides the total thickness interference fringes. The solid curve, shown in Fig. 3, is a dynamical simulation assuming the strain information obtained from the map and the elastic constants from the literature.[10] The values of the elastic constants used for PbTe were $c_{11}=108$, $c_{12}=7.7$, and $c_{44}=13.4$ and for SnTe, $c_{11}=109$, $c_{12}=2.1$, and $c_{44}=9.7$, in GPa. The agreement is remarkably good in the position and intensities of all features. The layer thicknesses obtained from the simulation are 174 Å for PbTe and 17 Å for SnTe, also in good agreement with nominal values. The FWHM for all SL peaks are the same, and is determined by the finite thickness of the SL, indicating that interdiffusion is very low and thickness reproducibility from layer to layer is also very good.

Figures 4(a) and 4(b) show the (224) reciprocal space map of two free-standing PbTe/SnTe SLs. In both samples, the PbTe layer has a nominal thickness of 225 Å, while the SnTe thickness is 70 Å [sample MBE160, Fig. 4(a)] and 130 Å [sample MBE161, Fig. 4(b)]. The PbTe and SnTe layers were repeated 50 times. The two dashed lines in each figure indicate the alignments of the peaks belonging to the SL and the PbTe buffer. It is clear, that in both samples, SL and buffer do not have the same in-plane lattice parameter. As the average SnTe content in the SL increases one can observe an increase in the horizontal separation between the SL and buffer layer peaks, reflecting the increase in SL relaxation. The in-plane strain between SL and buffer is defined as $(a_{\parallel SL}-a_{\parallel Buff})/a_{\parallel Buf}$, where $a_{\parallel Buff}$ and $a_{\parallel SL}$ are the in-plane lattice constants of buffer and SL, respectively, and can be obtained from the map. The strains, determined directly from distance between the dashed lines for each sample in Figs. 4(a) and 4(b), are -2.3×10^{-3} and -7.3×10^{-3}, for samples

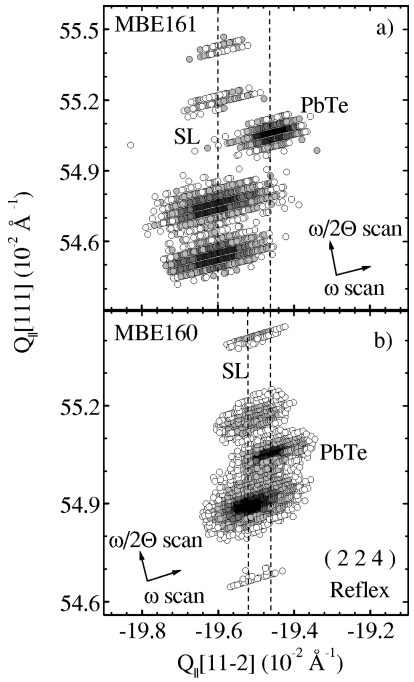

FIG. 4. Reciprocal space map around the (224) asymmetric Bragg diffraction point for two free-standing SLs. (a) Sample MBE160, with a SnTe layer thickness of 70 Å. (b) Sample MBE161, where the thickness of the SnTe layer is 130 Å. In both samples, the PbTe layer has a nominal thickness of 225Å and the PbTe and SnTe layers were repeated 50 times.

MBE160 and MBE161, respectively. It is important to note that, in contrast to the pseudomorphic sample, the FWHM in the ω direction of the free-standing SL peaks are even bigger than that of the PbTe buffer, due to defects introduced during the relaxation process.

The (222) diffraction spectra (points) and the result of the simulation (solid curve) for the sample MBE161 is shown in the Fig. 5. The thickness obtained from the simulation for PbTe and SnTe are 232 and 122 Å, respectively, showing a relatively good agreement with the nominal values. The results of the dynamical simulation of the free-

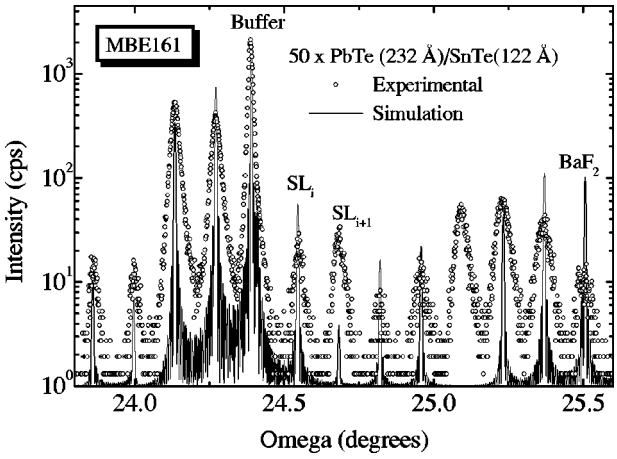

FIG. 5. X-ray data and simulation of the (222) $\omega/2\Theta$ scan for sample MBE161. In the simulation, the five first repetitions were assumed to be pseudomorphic, while the rest of the SL has a linear strain profile with a mean value of 7.05×10^{-3}, taken from Fig. 4(b).

standing SLs were worse when compared to the pseudomorphic samples. First, the strong modulation in the SL satellite intensities, observed for the free-standing samples, does not permit to identify the zero order satellite peak. Tentative simulations with the whole SL having only one in-plane lattice parameter, as expected from the free-standing assumption, do not give good results, even if we use the strain extracted from the map. This implies that the lattice constant changes within the SL. The best simulation fit, shown in Fig. 5, was obtained assuming that the first five repetitions of the SL are completely pseudomorphic to the buffer, while the rest have a linear strain profile with a mean value equal to that obtained from the map. The difference in the relative peak intensities between experimental points and simulation observed in Fig. 5 shows that the strain profile inside the sample is much more complex than our assumption. The larger FWHM of the measured data as compared to the simulation is a direct evidence of the dislocations introduced in the relaxation process.

V. CONCLUSIONS

We have shown that x-ray reciprocal space mapping is an essential technique for characterization of PbTe/SnTe superlattices. For SLs where the total thickness is small enough, we have shown that they are completely pseudomorphic to the buffer. Dynamical simulations show that almost perfect samples, with very small interdiffusion, if any, can be grown by MBE. In these samples, the strain state is completely determined. On the other hand, for thicker SLs, the map shows that they start to relax, having an in-plane lattice constant different from the buffer. In such samples, although the individual layers are below the critical thickness, defects are introduced due to the relaxation process of the entire SL. Besides that, a very complex strain profile is present within the SL and the simulations indicate that part of the SL is still pseudomorphic.

From these results we can conclude that for SLs grown directly on BaF_2 or KCl, without using a buffer layer (this is the case of almost all samples studied by other authors until now) the situation must be even more dramatic, since the lattice constant mismatch between the SL and substrate is larger than the one between SL and the PbTe buffer. Therefore, any tentative explanation of the results of electrical or optical measurements for such samples must take into account the strain profile in the sample. Besides that, quantitative determination of the strain profile for such samples seems to be a very complicated task and more work must be done in this field to understand how relaxation occurs in this system.

ACKNOWLEDGMENTS

The authors would like to thank the ''Conselho Nacional de Desenvolvimento Científico e Tecnológico (CNPq),'' Project Nos. 301091/95-1 and 300397/94-1 and the ''Fundação de Amparo à Pesquisa do Estado de São Paulo (FAPESP),'' Project Nos. 96/4546-0 and 95/6219-4 for the financial support of this work.

[1] K. Murase, S. Ishida, S. Takaoka, and T. Okumura, Surf. Sci. **170**, 486 (1986).
[2] M. A. Tamor, H. Holloway, L. C. Davis, R. J. Baird, and R. E. Chase, Superlattices Microstruct. **4**, 493 (1988).
[3] O. A. Mironov, O. N. Makarovskii, O. N. Nashchekina, L. P. Shpakovskaya, V. I. Litvinov, M. Oszwaldovski, and T. Berus, Acta Phys. Pol. A **88**, 853 (1995).
[4] V. Litvinov, M. Oszwaldowski, T. Berus, and O. Mironov, Phys. Status Solidi A **145**, 503 (1994).
[5] E. Abramof, S. O. Ferreira, P. H. O. Rappl, H. Closs, and I. N. Bandeira, J. Appl. Phys. **82**, 2405 (1997).
[6] P. H. O. Rappl, H. Closs, S. O. Ferreira, E. Abramof, C. Boschetti, P. Motisuke, A. Y. Ueta and I. N. Bandeira, J. Cryst. Growth (in press).
[7] A. I. Fedorenko, O. N. Nashchekina, B. A. Savitskii, and L. P. Shpakovskaya, Vacuum **43**, 1191 (1992).
[8] P. F. Fewster, Semicond. Sci. Technol. **8**, 1915 (1993).
[9] E. Koppensteiner, G. Bauer, H. Kibbel, and E. Kasper, J. Appl. Phys. **76**, 3489 (1994).
[10] G. Nimtz, in *Numerical Data and Functional Relationships in Science and Technology*, edited by K. Hellwege and O. Madelung, Landolt-Bönrstein, New Series Group III, Vol. 17 Part F (Springer, Berlin, 1993), pp. 146 and 168.